JOURNAL OF THERMOPHYSICS AND HEAT TRANSFER
Vol. 16, No. 3, July–September 2002

Three-Dimensional Discrete Ordinates Method in Transient Radiative Transfer

Zhixiong Guo*
Rutgers University, Piscataway, New Jersey 08854
and
Sunil Kumar†
Polytechnic University, Brooklyn, New York 11201

A complete transient three-dimensional discrete ordinates method is formulated for the first time to solve transient radiative transfer in a rectangular enclosure containing nonhomogeneous media that absorb, emit, and scatter. Twofold validation of the transient method is obtained: First, there is an excellent agreement between its results at long time stage with several steady-state solution methods. Second, the transient predictions of transmittance and reflectance compare very well with Monte Carlo simulations. The sensitivity and accuracy of the transient method against the sizes of time increment and grid cell and angular discrete order are examined. The false radiation propagation and numerical diffusion associated with the differencing schemes are discussed. Calculations show the behavior of the wave nature of propagation of transient radiation. The transient behavior of radiation is found to be influenced by many parameters, such as the boundary conditions, the optical thickness of the medium, the scattering albedo, and the incident radiation pulse width. Duhamel's superposition theorem is also applied to obtain the transient response to different temporal input pulses.

Nomenclature

A	=	area
c	=	speed of light
E_b	=	blackbody emissive power
G	=	incident radiation
$H(t)$	=	Heaviside unit step function
I	=	radiation intensity
L, H, W	=	length, height, and width
N	=	angular discrete order in S_N approximation
n	=	number of angular discretization
Q	=	radiative heat flux
R	=	reflectance
$\boldsymbol{r}$	=	position vector
S	=	source term
T	=	transmittance
t	=	time
t_p	=	pulse width
V	=	volume
W	=	angular weight
x, y, z	=	space coordinates
γ	=	weighting factor
Δt	=	time step
Δx	=	grid size
ξ, η, μ	=	direction cosines
ρ	=	reflectivity
σ_a	=	absorption coefficient
σ_e	=	extinction coefficient
σ_s	=	scattering coefficient
Φ	=	scattering phase function
ω	=	scattering albedo

Subscripts

d	=	downstream
P	=	control volume index
u	=	upstream
w	=	wall

Superscripts

l	=	control angle index
$*$	=	dimensionless quantity

Received 23 March 2001; revision received 14 June 2001; accepted for publication 11 March 2002.

*Assistant Professor, Department of Mechanical and Aerospace Engineering.

†Associate Professor and Othmer Senior Fellow, Department of Mechanical Engineering, 6 Metrotech Center; skumar@poly.edu. Senior Member AIAA.

I. Introduction

INTEREST in the study of transient radiative transfer has been increasing in recent years mainly because of the applications of short pulse lasers in a variety of engineering and biomedical problems, such as laser ablation,[1] optical tomography,[2] laser–tissue interaction,[3] laser material processing of microstructures,[4] and others. The transient nature of radiation transport in such applications is introduced via the inclusion of time derivative in the radiative transfer equation that accounts for the speed of radiation propagation. Some unique features associated with the transient radiation are being exploited and becoming well known, such as the thermal wave induced by pulsed laser heating[5] and the broadening of reflected and transmitted pulses after a laser pulse passes through a scattering medium.[6] Besides these emerging technologies, transient radiative transfer is also of significant in traditional applications, for instance, in astrophysical radiation hydrodynamics,[7] where the physical domain is very large. Note that the transient radiative transfer in the present study includes not only the transient boundary conditions as is done in the traditional concept of transient transfer,[8] but most important, it also incorporates the effect of radiation propagation speed in the governing equations.

The transient effects due to the speed of radiation propagation are only important for times of the order the characteristic time of travel of radiation along a characteristic path length within the geometry under consideration. A typical order of magnitude of this characteristic time can be estimated by dividing the characteristic length with the speed of propagation (which is the speed of light in the particular medium). For applications such as tissues where the characteristic length varies from few millimeters to dozens of

millimeters, the corresponding characteristic time is of the order of 10–100 ps. With the advent and utilization of lasers with pulse widths as short as 5 fs, the inclusion of the effects of propagation speed are needed for such applications.

Another characteristic of ultrashort pulse applications is that emission from the media can be neglected and each medium can be considered to be a cold medium. This is due to the small amount of energy deposited per pulse, which is not enough to raise the temperature significantly, and any emission can be neglected in comparison to the intensity of the scattered incident pulse. Additionally, any emission from the medium will be at higher wavelengths due to the low medium temperatures and need not be included in the monochromatic analysis conducted at the wavelength of the laser. Heat diffusion and heat capacity are also not significant at the short timescales considered.

The modeling of three-dimensional radiative transfer is usually a formidable task even in steady state because it involves solving integro–differential equations. The addition of the transient term in transfer equation further increases the complexity of modeling. There are mainly two categories in the modeling of transient radiative transfer, namely, the stochastic approaches and the deterministic. The stochastic Monte Carlo method is usually adopted for the simulation of short pulse laser propagation because it avoids the handling of the complicated integro–differential relationship, is flexible to deal with realistic physical conditions, and is algorithmically simple. Wilson and Adam[3] were among the first to study the propagation of light in tissue using the Monte Carlo model. After that, a number of researchers employed the Monte Carlo method in the study of transient laser radiation transfer.[9] Recently, Guo et al.[6] have developed the Monte Carlo method for multidimensional geometries that incorporates the Gaussian temporal and spatial characteristics of lasers. The shortcomings of the Monte Carlo method are that it is time-consuming and that the results are subject to statistical error due to practical finite samplings. In brain tumor diagnosis, for example, the nondimensional optical thickness of the tissue is usually over 100, the ballistic component of the laser beam passing through the tissue is then in the order of e^{-100}, which is too small to be captured precisely by the Monte Carlo method even with the use of a huge number of samplings.

In contrast, the deterministic approaches do not suffer such defects. Among the several deterministic methods adopted in the solution of transient radiative transfer, Rackmil and Buckius[10] proposed the adding–doubling method to solve transient response of a medium with a unit-step external source. Kumar et al.[11] employed the P_1 model to solve the parabolic and hyperbolic one-dimensional transient transfer equation. Mitra et al.[12] further developed the P_1 model to a two-dimensional rectangular enclosure. More recently, Mitra and Kumar[13] examined the discrete ordinates method, the P_1 and P_3 models, diffuse approximation, and two-flux method for short pulse laser transport in one-dimensional planar medium and found that the discrete ordinates method predicts more accurate transient results. After that, Tan and Hsu[14] and Wu and Wu[15] separately developed integral formulation for transient radiative transfer in one- and two-dimensional geometries. Guo and Kumar[16] extended the radiation element method to transient radiative transfer. The discrete ordinates method has been applied to study short pulsed laser interaction and transport in two-dimensional enclosures of biological tissues.[17] However, a literature survey reveals that no discrete ordinates method is available for solving the transient transfer equation in three-dimensional configurations.

Significant progress has been made in the development of solving three-dimensional steady-state radiative transfer in recent decades. Examples are the Monte Carlo method,[18] the discrete ordinates method,[19] the finite volume method,[20] the YIX method,[21] the P_3 model,[22] and the radiation element method (REM),[23] to name a few. Among them, the discrete ordinates method (DOM) has been one of the most widely applied methods because it requires a single formulation to invoke higher-order approximations of discrete ordinate quadrature sets, integrates easily into control volume transport codes, and is applicable to the complete anisotropic scattering phase function and inhomogeneous media.

In the present study, the DOM is formulated for transient radiative transfer in three-dimensional rectangular enclosures that contain inhomogeneous absorbing, emitting, and scattering media. The resulting transient DOM (TDOM) is validated by comparing with Monte Carlo simulations and by comparing the long-time results with published steady-state values for selected cases. Excellent agreement is found in all cases considered, instilling confidence in the TDOM model developed.

To test the TDOM method, the cases considered are simple hypothetical ones. They are chosen to have the smallest number of parameters so that the TDOM method and its features can be highlighted and comparisons with other methods can be made without being obscured by large number of parameters and their possible range of values. It is for this reason that simple boundary driven and volumetric source driven problems are studied. Specifically, the two cases considered are the study of transient and steady behavior of radiative heat transfer in a three-dimensional enclosure with cold walls and a cube with inhomogeneous medium that is instantaneously heated at the first instant of the problem. The first case is a simplified depiction of laser irradiation being treated as a boundary condition, and the second is chosen primarily to compare with benchmark steady-state results published.[21] Detailed models related to thin collimated pulsed laser beams are not considered in this first study of TDOM because they would introduce several additional parameters that should be considered only after the method has been established.

The influences of the sizes of time step and cell grid and the angular discrete order in the TDOM method are examined. New concepts, not occurring in steady-state DOM are introduced, such as time step limitation and wave nature. False radiation propagation associated with finite differencing numerical implementation of the wave characteristics associated with the hyperbolic nature of the transient radiative transfer equation is discussed. The influences of optical thickness, scattering albedo, boundary reflectivity, and incident pulse width are scrutinized. Duhamel's superposition theorem is applied to obtain the transient response of pulsed radiation and is validated by comparison with the results from direct simulation of pulsed radiation.

II. Mathematical Models

A. Transfer Equations

In a three-dimensional rectangular enclosure as shown in Fig. 1, the transient radiative transfer equations in discrete ordinates form can be formulated as

$$\frac{1}{c}\frac{\partial I^l}{\partial t} + \xi^l \frac{\partial I^l}{\partial x} + \eta^l \frac{\partial I^l}{\partial y} + \mu^l \frac{\partial I^l}{\partial z} + \sigma_e I^l = \sigma_e S^l, \qquad l = 1, 2, \ldots, n \quad (1)$$

where ξ^l, η^l, and μ^l are the three direction cosines in a discrete ordinate direction $\hat{s}^l$ and I^l is the radiation intensity in the direction and is a function of position (x, y, z) and time t. The extinction coefficient σ_e is the sum of absorption coefficient σ_a and scattering coefficient σ_s. The speed of light in the medium is c. S^l is the radiative source term and can be expressed as

$$S^l = (1-\omega)I_b + \frac{\omega}{4\pi}\sum_{i=1}^{n} w^i \Phi^{il} I^i, \qquad l = 1, 2, \ldots, n \quad (2)$$

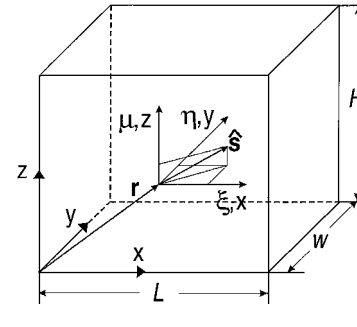

Fig. 1 Geometry and coordinate system.

where scattering albedo $\omega = \sigma_s/\sigma_e$ and Φ^{il} represents the scattering phase function $\Phi(\hat{s}^i \to \hat{s}^l)$. A quadrature set of n discrete ordinates with the appropriate angular weight w^l, $l = 1, 2, \ldots, n$, is used in the S_N approximation[24,25] and $n = N(N+2)$. The scattering phase function may be approximated by a finite series of Legendre polynomials as

$$\Phi^{il} = \sum_{k=0}^{M} C_k P_k(\cos\varphi^{il}) \tag{3}$$

and the argument can be obtained as

$$\cos\varphi^{il} = \hat{s}^i \cdot \hat{s}^l = \xi^i\xi^l + \eta^i\eta^l + \mu^i\mu^l \tag{4}$$

The C_k are the expansion coefficients of the corresponding Legendre functions P_k. For isotropic scattering phase function, $\Phi^{il} \equiv 1$.

The enclosure walls are assumed to be gray and diffusely reflecting. The diffuse intensity at the wall of $x = 0$ is

$$I_w = (1-\rho_w)I_{bw} + \frac{\rho_w}{\pi}\sum_{\xi^l<0}^{n/2} w^l I^l |\xi^l| \tag{5}$$

where ρ_w is the diffuse reflectivity of the wall surface. Similarly, the relationships for the rest five walls can be set up.

Once the intensity field is obtained, the incident radiation G, the net radiative heat fluxes Q_x, Q_y, and Q_z, and the divergence of radiative heat flux $\nabla \cdot \boldsymbol{q}$ can be calculated as

$$G = \sum_{l=1}^{n} w^l I^l \tag{6}$$

$$Q_x = \sum_{l=1}^{n} \xi^l w^l I^l, \qquad Q_y = \sum_{l=1}^{n} \eta^l w^l I^l, \qquad Q_z = \sum_{l=1}^{n} \mu^l w^l I^l \tag{7}$$

$$\nabla \cdot \boldsymbol{q} = \kappa(4E_b - G) \tag{8}$$

where E_b is the blackbody radiative emissive power of the medium.

In boundary-driven problems in which a wall is the source of a suddenly imposed (at $t = 0^+$) emitting power E_0, the reflectance at the incident wall $x = 0$, and the transmittance at opposite output wall, $x = L$, are defined as

$$R(y,z,t) = \frac{(1-\rho_w)}{E_0}\sum_{\xi^l<0}^{n/2} |\xi^l| w^l I^l(x=0,y,z,t)$$

$$T(y,z,t) = \frac{Q_x(x=L,y,z,t)}{E_0} \tag{9}$$

Note that all of the variables are time dependent in the present study.

B. Duhamel's Superposition Theorem

Duhamel's theorem is popularly used in the solution of heat conduction problems with time-dependent boundary conditions and/or time-dependent heat generation by relating them to the solution of the same problem with time-independent boundary conditions and/or heat generation. The description of the theorem can be found in heat conduction textbooks.[26] Here we apply Duhamel's theorem to the solution of transient radiative transfer problems with time-dependent boundary conditions.

Consider a space region: One part of the boundary of the region is subject to a time-dependent radiation pulse $f(t)$. (It can be of any form, either continuous or discontinuous.) The remaining portions of the boundary and the medium in the region are cold. Let $\theta(\boldsymbol{r}, t)$ be the solution of the same problem with the assumption of a time-independent unit step radiation pulse on that boundary. Here, $\theta(\boldsymbol{r}, t)$ could be reflectance, transmittance, surface heat flux, and/or divergence of heat flux. Duhamel's theorem relates the solution $\Theta(\boldsymbol{r}, t)$ of the problem subject to the time-dependent pulse $f(t)$ to $\theta(\boldsymbol{r}, t)$ which is the solution of the problem subject to a unit step radiation at time $t = 0$ by the following integral expression[26]:

$$\Theta(\boldsymbol{r}, t) = \int_{\tau=0}^{t} f(\tau)\frac{\partial\theta(\boldsymbol{r}, t-\tau)}{\partial t}\,\mathrm{d}\tau \tag{10}$$

If the boundary is subject to a square radiation pulse, that is,

$$f(t) = H(t) - H(t - t_p) \tag{11}$$

the solution of the time-dependent pulse response is simply obtained as

$$\Theta(\boldsymbol{r}, t) = \theta(\boldsymbol{r}, t) - \theta(\boldsymbol{r}, t - t_p) \tag{12}$$

Note that Duhamel's theorem can only be applied to linear systems. The transient radiative transfer equation [see Eq. (1)] is linear when only the radiation intensity is considered as is done in the cases studied in the present paper where emission is neglected. Because most transient radiative transfer problems deal with ultrashort timescales and address the propagation of pulsed radiation, the medium emission is usually negligible, or the temperature of the medium is treated as unchanged during the very short time of the application. Thus, Duhamel's theorem is generally applicable to ultrafast laser radiation propagation.

C. Numerical Schemes

To solve the transfer equation (1) in discrete ordinates method, the enclosure is divided into a number of small control volumes in an orthogonal grid. With the exception of the transient time term, Eq. (1) has been spatially discretized in multidimensional rectangular configuration by many researchers.[19,24] With the addition of discretization in timescale, the transfer equation can be expressed as

$$(V/c\Delta t)\left(I_P^l - I_P^{l0}\right) + |\xi^l|\left(A_{xu}I_{xu}^l - A_{xd}I_{xd}^l\right) + |\eta^l|\left(A_{yu}I_{yu}^l - A_{yd}I_{yd}^l\right) + |\mu^l|\left(A_{zu}I_{zu}^l - A_{zd}I_{zd}^l\right) = \sigma_{eP}V\left(-I_P^l + S_P^l\right) \tag{13}$$

where $A_{xu} = A_{xd} = \Delta y\Delta z$, $A_{yu} = A_{yd} = \Delta x\Delta z$, $A_{zu} = A_{zd} = \Delta x\Delta y$, and $V = \Delta x\Delta y\Delta z$. I_{xd}^l, I_{yd}^l, and I_{zd}^l are the radiation intensities on the downstream surfaces in the $\hat{s}^l$ direction. I_{xu}^l, I_{yu}^l, and I_{zu}^l are those on the upstream surfaces in the direction. Subscript P denotes the nodal of the control volume. I_P^{l0} is the radiation intensity in the previous time step. A zero initial intensity field is assumed in the present study. S_P^l is calculated from Eq. (2) as

$$S_P^l = (1-\omega)I_{bP} + \frac{\omega}{4\pi}\sum_{i=1}^{n} w^i\Phi^{il}I_P^i \tag{14}$$

To solve Eq. (13), the weighted finite differencing scheme is usually used to relate the radiation intensities on the cell surfaces with those at the cell centers:

$$I_P^l = \gamma_x^l I_{xd}^l + (1-\gamma_x^l)I_{xu}^l = \gamma_y^l I_{yd}^l + (1-\gamma_y^l)I_{yu}^l = \gamma_z^l I_{zd}^l + (1-\gamma_z^l)I_{zu}^l \tag{15}$$

For the determination of the values of weights γ_x^l, γ_y^l, and γ_z^l, the positive scheme proposed by Lathrop[27] is applied in the present study:

$$\gamma_x^l = \max\left(0.5, 1 - \frac{|\xi^l|/\Delta x}{2(|\eta^l|/\Delta y + |\mu^l|/\Delta z) + \sigma_e}\right) \tag{16a}$$

$$\gamma_y^l = \max\left(0.5, 1 - \frac{|\eta^l|/\Delta y}{2(|\xi^l|/\Delta x + |\mu^l|/\Delta z) + \sigma_e}\right) \tag{16b}$$

$$\gamma_x^l = \max\left(0.5,\ 1 - \frac{|\mu^l|/\Delta z}{2(|\xi^l|/\Delta x + |\eta^l|/\Delta y) + \sigma_e}\right) \quad (16c)$$

The final discretization equation for the cell intensity in a generalized form becomes

$$I_P^l = \frac{(1/c\Delta t)I_P^{l0} + \sigma_e S_P^l + (|\xi^l|/\gamma_x^l \Delta x)I_{xu}^l + (|\eta^l|/\gamma_y^l \Delta y)I_{yu}^l + (|\mu^l|/\gamma_z^l \Delta z)I_{zu}^l}{1/c\Delta t + \sigma_e + |\xi^l|/\gamma_x^l \Delta x + |\eta^l|/\gamma_y^l \Delta y + |\mu^l|/\gamma_z^l \Delta z} \quad (17)$$

Equation (15) is used to solve for the downstream boundary intensities, with the nodal intensity obtained from Eq. (17). When compared with the conventional DOM forms in steady-state transfer problems, the TDOM forms have introduced the time discretization terms in Eq. (17), and all of the variables there may be time dependent. When the time step is set to be infinitely large, the transient formulation asymptotes to steady state. Hence, the present formulation is feasible for the analyses of both transient and steady-state radiation transfer.

The present formulation has first-order accuracy in the time and spatial domains. This ensures that the numerical results would not be oscillatory. However, such a treatment induces strong numerical diffusion. Such characteristics have been broadly discussed in the solution of wave equations in conventional computational fluid dynamics (CFD).[28] To minimize the numerical diffusion, the spatial grid and the time step are required to be as fine as possible. As a result, this increases CPU time. There should be a compromise between computation cost and the refinement of spatial and time grids.

Fiveland suggests that the spatial differential step satisfy the conditions[19,25]

$$\Delta x < |\xi^l|_{\min}/\sigma_e\left(1 - \gamma_x^l\right), \qquad \Delta y < |\eta^l|_{\min}/\sigma_e\left(1 - \gamma_y^l\right)$$
$$\Delta z < |\mu^l|_{\min}/\sigma_e\left(1 - \gamma_z^l\right) \quad (18)$$

For transient analysis, a condition on the time step should also be imposed. Because a light beam always travels in the speed of light c, the traveling distance $c\Delta t$ between two neighboring time steps should not exceed the size of cell grid, that is, $c\Delta t < \min\{\Delta x, \Delta y, \Delta z\}$. If we define dimensionless variables $t^* = ct/L$, $x^* = x/L$, $y^* = y/L$, and $z^* = z/L$, we have

$$\Delta t^* < \min\{\Delta x^*, \Delta y^*, \Delta z^*\} \quad (19)$$

The time step condition of Eq. (19) is relatively easier to be satisfied. As pointed out by Fiveland,[25] however, it may not be practical to satisfy Eq. (18) due the limitation of computer memory. Particularly in three-dimensional configuration, the radiation intensity is not only a function of three spatial dimensions but is also discretized in the angular direction. In the case of S_{12} quadrature, for example, the angular dimension is as large as $n = 12(12+2) = 168$. That is equivalent to the solution of 168 coupled equations in three-dimensional CFD.

The choice of quadrature scheme in DOM method is arbitrary and studies on the quadrature selection have been made by a number of researchers.[25] In the present study, the quadrature sets and corresponding angular weights are taken from the code TWOTRAN[29] for S_{14} and S_{16} approximations. The quadrature sets and corresponding angular weights for S_8 and S_{12} approximations can be found by Fiveland.[25] In general, the S_{12} approximation is adopted in the calculations if not specifically mentioned.

In the present computations, a personal computer with one CPU of Pentium III 500-Hz xeon was used. It takes several minutes to dozens of hours in calculation depending on the specified problem and the size of grid.

III. Comparison with Published Steady-State Benchmark

As discussed earlier, one of the cases selected for study is a unit cube considered by Hsu and Farmer[21] as a benchmark for comparison of steady-state results. To validate the present method, the TDOM approach is first applied to a similar unit cube, which contains inhomogeneous media. The distribution of the inhomogeneous nature is represented by the variation of the optical thickness in the media that was selected by Hsu and Farmer[21] and is given by

$$\tau(x, y, z) = a\left(1 - \frac{|x - 0.5|}{0.5}\right)\left(1 - \frac{|y - 0.5|}{0.5}\right)\left(1 - \frac{|z - 0.5|}{0.5}\right) + b \quad (20)$$

The constants in Eq. (20) are given as $a = 0.9$ and $b = 0.1$. The walls are cold, black, and diffuse. To compare our transient prediction with the existing steady-state results from the literature,[21] we assume that a unity blackbody emissive power be instantaneously assigned to the hot media. Although such a physical case can be taken to be unrealistic for transient radiation, its purpose is for numerical comparison with the published benchmark results. Two cases are selected for the present study: case E1, purely absorbing–emitting media ($\omega = 0$) and case E2, absorbing, emitting, and isotropically scattering media ($\omega = 0.9$). In all computations in this subsection, a $9 \times 9 \times 9$ cubic grid with a uniform control volume width ($\Delta x^* = \Delta y^* = \Delta z^* = \frac{1}{9}$) is adopted. The surface heat flux and divergence of heat flux are to be evaluated as a function of time.

The temporal behavior is shown in Fig. 2 for the case of E1. The effect of the size of time step is examined. It is seen that, as time proceeds, the divergence of heat flux (at the center of the cube) decreases and gradually reaches a constant value, while the surface heat flux (at the location $x = z = 0.5$, $y = 0$) increases but also reaches a constant value. Both the constant values of surface heat flux and divergence of heat flux are the solutions of the TDOM at steady state, and it is observed that the constant values at the long time stage are not affected by the size of the time step. However, the size of time step does affect the transient behavior of surface heat flux and divergence of heat flux. It is found that when Eq. (19) is violated, that is, when $\Delta t^* > \Delta x^*$, such as in the cases of $\Delta t^* = 0.15$ and 0.30 (for $\Delta x^* = \frac{1}{9} = 0.111$), steady-state values are reached that match all others. However, the errors in the transient regime are significant, and the predicted heat flux and its divergence deviate from those predicted by smaller time steps. The temporal development

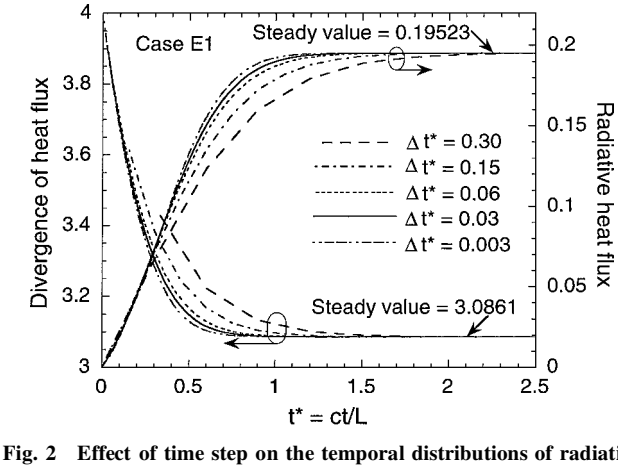

Fig. 2 Effect of time step on the temporal distributions of radiative heat flux and divergence of heat flux in a unit cube with hot media.

Table 1 Comparisons of divergences of radiative heat flux along the centerline ($y = z = 0.5$) for steady state between present TDOM and published YIX and MC[21]

	Case E1			Case E2		
Position	TDOM	YIX	MC	TDOM	YIX	MC
0	3.0885	3.0366	3.0981	0.38930	0.38842	0.39192
1/9	2.5325	2.4963	2.5364	0.31224	0.31163	0.31433
2/9	1.9778	1.9566	1.9836	0.23517	0.23482	0.23482
3/9	1.3817	1.3721	1.3874	0.15755	0.15739	0.15866
4/9	0.72452	0.72219	0.72910	0.079171	0.079120	0.079740

Table 2 Comparisons of radiative heat flux at surface ($y = 0, z = 0.5$) for steady state between present TDOM and published YIX and MC[21]

	Case E1			Case E2		
Position	TDOM	YIX	MC	TDOM	YIX	MC
0	0.19523	0.19291	0.19260	0.022174	0.021920	0.022020
1/9	0.18557	0.18569	0.18552	0.021022	0.021070	0.021030
2/9	0.16672	0.16619	0.16729	0.018788	0.018770	0.018920
3/9	0.14143	0.14171	0.14125	0.015840	0.015890	0.015640
4/9	0.11143	0.10872	0.10959	0.012420	0.012140	0.012190

with increasing time is slower for the large time step cases. When $\Delta t^* < \Delta x^*$, converged transient results are found for the selected three cases ($\Delta t^* = 0.06$, 0.03, and 0.003). The differences between the predictions of $\Delta t^* = 0.03$ and 0.003 are slight in the transient domain.

The divergences of radiative heat flux along the centerline ($y = z = 0.5$) and the surface radiative heat fluxes at the surface ($y = 0$, $z = 0.5$) predicted by the TDOM at long time are compared with the published data of steady-state solutions by the YIX and Monte Carlo (MC) methods[21] in Tables 1 and 2, respectively. The transient divergences and heat fluxes reach steady-state results very quickly, in less than $t^* = 2$. The differences between the TDOM and steady-state YIX and between the TDOM and steady-state MC are generally less than 1%.

IV. Results of Numerical Implementation and Parametric Sensitivity

The simplified, reduced parameter, physical case of a three-dimensional geometry in Cartesian coordinates is considered in this section, where one wall is hot and the others are cold. The homogeneous scattering medium is also cold. This configuration is a simplified depiction, where the hot wall represents a laser source that is treated as a boundary condition. This case is chosen because it is the simplest one that permits sensitivity studies of intrinsic parameters related to numerical implementation, such as discretization intervals and number of ordinates, to be conducted without being obscured by other parameters related to lasers, etc., that would be needed to achieve a more accurate description of the laser incidence.

A. Cube with One Hot Wall

In this subsection, transient transfer is investigated in a unit cube with one hot wall, at $x = 0$, of instantaneously assigned unity blackbody emissive power representing the sudden incidence of a laser pulse. The homogeneous medium is purely scattering and cold. The remaining walls are black and cold. As already indicated, the physical model addresses the ultrafast laser propagation in material by treating the laser as a boundary condition via a transient hot wall. The unit cube is divided into either $9 \times 9 \times 9$ cell grid with $\Delta x^* = \Delta y^* = \Delta z^* = \frac{1}{9}$ or $25 \times 25 \times 25$ cell grid with $\Delta x^* = \Delta y^* = \Delta z^* = 0.04$.

Figures 3 and 4 show the effects of control volume size and time step on the temporal distributions of transmittance and reflectance, respectively. The transient predictions by TDOM are compared with that by the MC method. The MC results in Figs. 3 and 4 are calculated based on the transient algorithm developed by the authors.[6] It is seen that both the transmittance and reflectance converge to

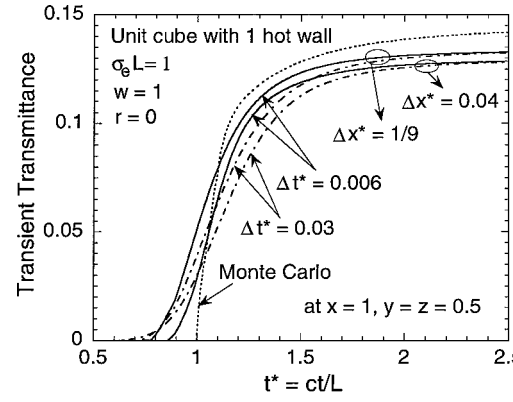

Fig. 3 Influences of time step and spatial grid on the temporal behavior of transmittance in a unit cube with one hot wall.

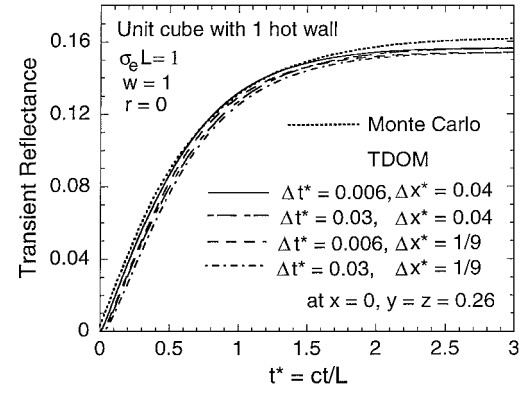

Fig. 4 Influences of time step and spatial grid on the temporal profile of reflectance in a unit cube with one hot wall.

constant values at the long time stage. Such constant values are independent of the size of time step but depend on the control volume grid. However, the differences of the constant values between the $\Delta x^* = 0.04$ grid and the $\Delta x^* = \frac{1}{9} = 0.111$ grid are not appreciable. The differences of the constant values between the TDOM and MC predictions are in the range of $5 \sim 15\%$, and the difference is more obvious for transmittance. This may be caused by the ray effect associated with the DOM method as explained in steady-state analysis.[29]

In Fig. 3, it is obvious that the transient behavior of transmittance is strongly affected by the grid division and time step. The transient transmittance predicted with the grid of $\Delta x^* = \frac{1}{9} = 0.111$ rises faster than that of $\Delta x^* = 0.04$. This is because the use of finite differencing scheme in Eq. (15) that relates the intensities at cell surfaces with those at cell centers assumes an infinite speed of radiation propagation. The larger the control volume size, the stronger is the false radiation propagation. Numerical diffusion also exists due to the spatial and temporal discretization in the transfer equation. The larger are the sizes of time increment and control volume grid, the more intense is the numerical diffusion. To minimize the numerical diffusion, it is better to use a finer grid and a smaller time step. However, even in the case of $\Delta x^* = 0.04$ and $\Delta t^* = 0.006$ as shown in Fig. 3, the numerical diffusion phenomenon still exists. The numerical diffusion cannot be eliminated no matter how fine the spatial and temporal grids are. It is found that the TDOM method cannot capture the abrupt rise of transmittance in the very early time period as predicted by the MC method. Such characteristics are very similar to the solution of wave equations in CFD.[28] As expected, no oscillations occurred in Figs. 3 and 4.

The influence of numerical diffusion is not so severe on the transient profile of reflectance as shown in Fig. 4. The transient distribution of reflectance predicted by the TDOM matches closely to that by the MC method. There might be two reasons. One is that the ray effect is not as strong in the hot wall as compared with the opposite

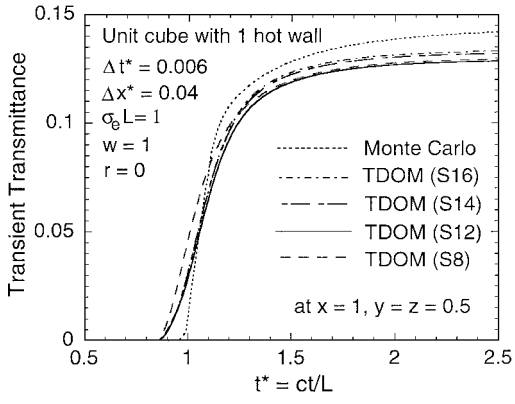

Fig. 5 Influence of angular discrete order on the temporal profile of transmittance in a unit cube with one hot wall.

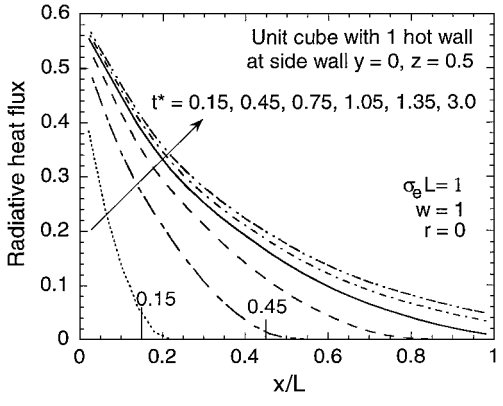

Fig. 6 Profiles of radiative heat flux along a sidewall at several time instants reflectance in a unit cube with one hot wall.

cold wall. Another reason is because the reflected radiation from the hot wall does not have to travel a long distance as does the transmitted radiation, so that the development of numerical diffusion with advancing the time and increasing the spatial distance is weaker.

The ray effect due to the finite discretization in the angular direction is usually stronger for transmittance in boundary-driven problems. To examine the ray effect in TDOM, the temporal profiles of transmittance predicted by various discrete approximations are compared in Fig. 5. The number of discrete ordinates associated with the S_N approximation is $n = N(N+2)$, for example, $n = 16(16+2) = 288$ for S_{16}. With the increase of discrete order N, the number of discrete ordinates, as well as the required CPU time and memory, increases, and the ray effect becomes weaker. It is seen from Fig. 5 that the S_{16} approach matches the MC simulation the best, whereas the S_8 has the worst match in the transient domain. However, it is observed that the increase of discrete order has no obvious effect on the improvement of false radiation propagation and numerical diffusion.

The profiles of surface radiative heat flux along one centerline in a sidewall ($y = 0$, $z = 0.5$) are shown in Fig. 6 for several time instants. As time elapses, it is seen that the surface heat fluxes increase and gradually reach constant values at the long time stage. The heat flux decreases as the location proceeds from smaller x (near the hot wall) to larger x. At early time instants, for example, $t^* = 0.15$, 0.45, and 0.75, it is seen that the heat flux is zero at locations $x^* > t^*$ because the radiation propagates with a speed of c and $x^* = x/L = ct/L = t^*$. The trait of wave propagation associated with the transient transfer analysis is clearly embodied. The small nonzero values in the locations $x^* > t^*$ are caused by the numerical diffusion as mentioned earlier.

B. Three-Dimensional Rectangular Enclosure with One Hot Wall

In this subsection, a parametric study is shown in Figs. 7–10 in a rectangular enclosure with $H = W = L/2$. The wall at $x = 0$ is suddenly subject to a laser irradiation that is treated in the model as a hot wall boundary condition. The medium and other five walls are cold. The hot wall, that is, subject to the incidence of laser, and the opposite output wall are black. The other four sidewalls are gray and diffuse with diffuse reflectivity ρ. The properties of the medium are homogeneous. In the calculations, the enclosure is divided into $50 \times 25 \times 25$ cell grid ($\Delta x^* = 0.02$) and the time step is $\Delta t^* = 0.006$.

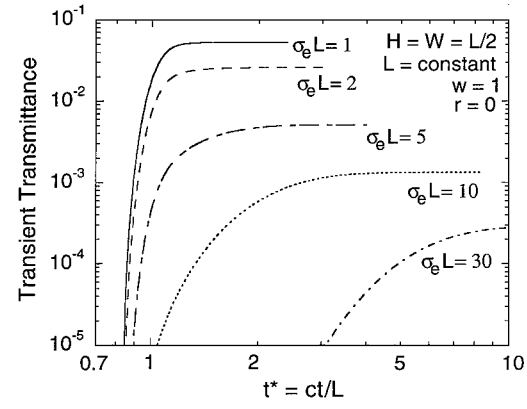

Fig. 7 Effect of optical thickness on the temporal profile of transmittance in a rectangular enclosure.

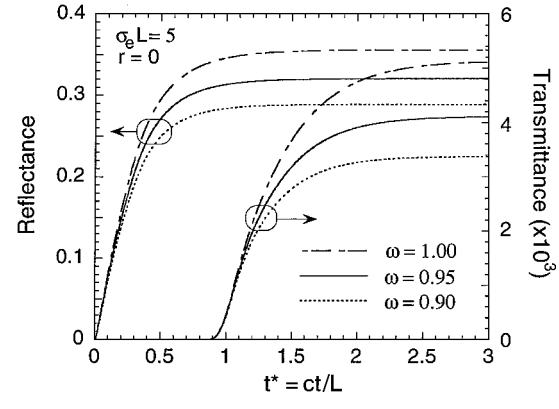

Fig. 8 Effect of scattering albedo on the temporal profiles of transmittance and reflectance in a rectangular enclosure.

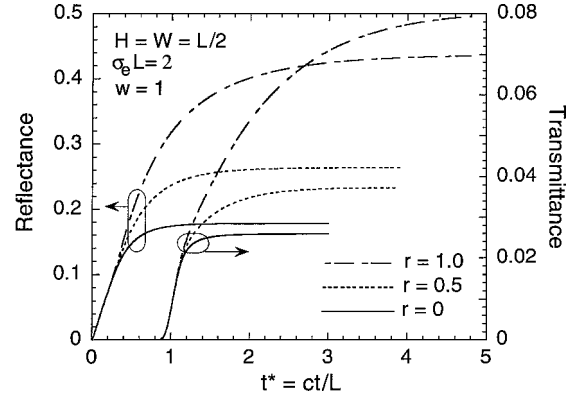

Fig. 9 Effect of surface reflectivity at sidewalls on the temporal profiles of transmittance and reflectance in a rectangular enclosure.

Figure 7 shows the temporal profiles of transmittance at the location $x = 1$, $y = z = 0.5$ for several selected optical depths. The optical thickness of the enclosure increases with the increase of the extinction coefficient of the medium. As the optical thickness increases, it is seen that the value of the transmittance decreases dramatically, the transmittance rises at some delayed time instants, the rising of the temporal transmittance becomes smoother, and the time needed to converge to a constant transmittance is longer. Such phenomena were explained by the increase of multiple scattering evens in MC simulation.[6]

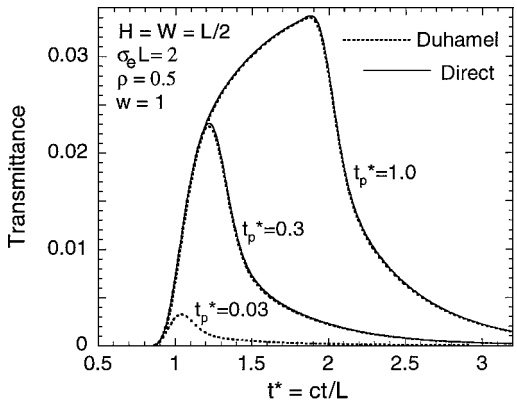

Fig. 10 Temporal distributions of transmittance subject to different incident radiation pulses: comparison between direct pulse simulation and use of Duhamel's theorem.

The influence of scattering albedo is demonstrated in Fig. 8, where the temporal distributions of transmittance and reflectance at the locations $y = z = 0.5$ are plotted for three selected values of scattering albedo. As expected, the magnitudes of transmittance and reflectance are strong functions of scattering albedo. With the decrease of albedo by 10% (from $\omega = 1$ to $\omega = 0.9$), the value of the transmittance at a long time instant decreases by nearly 50%. The decrease of scattering albedo also shortens the converging time, that is, the time when the transmittance and reflectance reach constant values. However, at early rising time period, the influence of scattering albedo is not obvious.

The effect of boundary condition is examined in Fig. 9, where three values of diffuse reflectivity at the sidewalls are chosen for comparison. In the case of $\rho = 0$, the sidewalls are black and absorb all incident radiation. When $\rho = 1.0$, the sidewalls do not absorb, but do reflect all incident radiation. It is seen that when the sidewalls are black, the temporal variation periods of transmittance and reflectance are much shorter than those when the sidewalls reflect radiation. With the increase of reflectivity in the sidewalls, the temporal variations of the transmittance and reflectance become longer and longer. In the case of $\rho = 1.0$, the transient profiles reach constant values very slowly, and the constant values are much larger than those of $\rho = 0$ and $\rho = 0.5$.

Finally, the transient transfer analysis of pulsed radiation is investigated in Fig. 10. The hot wall is subject to a square pulse with dimensionless pulse width $t_p^* = 0.03$, 0.3 and 1.0, respectively. The results marked as Direct in Fig. 10 are computed directly from the pulse boundary condition using TDOM. Those marked as Duhamel are the results calculated from the use of Duhamel's superposition theorem based on the solution of the same problem subjected to a unit step radiation. (See the result in Fig. 9 for the case of $\rho = 0.5$. All three Duhamel's results in Fig. 10 are based on that one solution.) It is seen that the pulsed responses integrated from Duhamel's superposition theorem match excellently the direct simulations. The slight difference can be attributed to the errors in the process of numerical integration. Hence, Duhamel's superposition theorem can be applied to the study of pulsed radiation propagation, and it saves computational resources and efforts because only one solution corresponding to a unit step radiation problem can be used for different problems subjected to various input pulse shapes and widths.

In Fig. 10, the broadening of the transmitted pulses is clearly seen. The long decaying tail is observed for the three selected incident pulses. When the incident square pulse width is $t_p^* = 0.03$, the transmitted pulse width (full width at half maximum) is larger than 0.1. With the increase of incident pulse width, the magnitude of the transmittance increases.

V. Conclusions

The discrete ordinates method is developed for the first time to study transient radiative transfer in three-dimensional rectangular enclosures of scattering, absorbing, and emitting media. The transient formulation is feasible for both transient and steady-state analyses. The results of this method match excellently with benchmark cases available in the literature for steady-state analysis. The predicted temporal distributions of transmittance and reflectance agree closely to those by MC simulation. To minimize the false radiation propagation due to weighted differencing scheme and the numerical diffusion due to finite difference, finer sizes of grid and time step are required. It is found that the dimensionless time step should be less than the dimensionless spatial grid. The ray effect can be improved by increasing the number of discrete ordinates. Some of the merits of the method in transient analysis are as follows: 1) It is well developed and commonly used in steady-state analysis. 2) It is algorithmically simple and compatible with CFD codes. 3) The requirement of computer resources is uncritical. 4) It can be used to deal with optically very thick medium. It also possesses the common merits and drawbacks of DOM method in steady-state analysis. An obvious disadvantage in transient analysis is that the numerical diffusion and false propagation are inevitable. This makes it difficult to capture precisely the abrupt rising of a transmitted radiation pulse.

Parametric studies show that with the increases of optical thickness, scattering albedo, and boundary reflectivity, the transient transmittance and reflectance develop more slowly, and they experience a longer time variation. In pulsed radiation transfer, this means that the transmitted pulse becomes wider. The temporal behavior is a function of medium optical thickness, scattering albedo, and boundary reflectivity. Duhamel's superposition theorem can be used to study pulsed radiation response subject to various incident pulse shapes.

Acknowledgments

The authors acknowledge partial support from Sandia National Laboratories–National Science Foundation joint Grant AW-9963 (CTS-973201) administered by Sandia National Laboratories, Albuquerque, New Mexico, Shawn Burns, Project Manager.

References

[1] Kumar, S., and Mitra, K., "Microscale Aspects of Thermal Radiation Transport and Laser Applications," *Advances in Heat Transfer*, Vol. 33, 1998, pp. 187–294.

[2] Yamada, Y., "Light–Tissue Interaction and Optical Imaging in Biomedicine," *Annual Review of Heat Transfer*, Vol. 6, 1995, pp. 1–59.

[3] Wilson, B. C., and Adam, G., "A Monte Carlo Model for the Absorption and Flux Distributions of Light Tissue," *Medical Physics*, Vol. 10, No. 6, 1983, pp. 824–830.

[4] Tien, C. L., Majumdar, A., and Gerner, F. M., *Microscale Energy Transport*, Taylor and Francis, Washington, DC, 1997.

[5] Chen, S. C., Grigoropoulos, C. P., Park, H. K., Kersterns, P., and Tam, A. C., "Photothermal Displacement Measurement of Transient Melting and Surface Deformation During Pulsed Laser Heating," *Applied Physics Letters*, Vol. 73, No. 15, 1998, pp. 2093–2095.

[6] Guo, Z., Kumar, S., and San, K.-C., "Multi-dimensional Monte Carlo Simulation of Short Pulse Laser Radiation Transport in Scattering Media," *Journal of Thermophysics and Heat Transfer*, Vol. 14, No. 4, 2000, pp. 504–511.

[7] Balsara, D. S., "An Analysis of the Hyperbolic Nature of the Equations of Radiation Hydrodynamics," *Journal of Quantitative Spectroscopy and Radiative Transfer*, Vol. 61, No. 5, 1999, pp. 617–627.

[8] Siegel, R., 1998, "Transient Thermal Effects of Radiant Energy in Translucent Materials," *Journal of Heat Transfer*, Vol. 120, No. 1, pp. 4–23.

[9] Flock, S. T., Patterson, M. S., Wilson, B. C., and Wyman, D. R., "Monte Carlo Modelling of Light Propagation in Highly Scattering Tissues—I: Model Predictions and Comparison with Diffusion Theory," *IEEE Transactions on Biomedical Engineering*, Vol. 36, No. 12, 1989, pp. 1162–1167.

[10] Rackmil, C. I., and Buckius, R. O., "Numerical Solution Technique for the Transient Equation of Transfer," *Numerical Heat Transfer*, Vol. 6, No. 2, 1983, pp. 135–153.

[11] Kumar, S., Mitra, K., and Yamada, Y., "Hyperbolic Damped-Wave Models for Transient Light-Pulse Propagation in Scattering Media," *Applied Optics*, Vol. 35, No. 19, 1996, pp. 3372–3378.

[12] Mitra, K., Lai, M.-S., and Kumar, S., "Transient Radiation Transport in Participating Media within a Rectangular Enclosure," *Journal of Thermophysics and Heat Transfer*, Vol. 11, No. 3, 1997, pp. 409–414.

[13] Mitra, K., and Kumar, S., "Development and Comparison of Models for Light-Pulse Transport Through Scattering–Absorbing Media," *Applied Optics*, Vol. 38, No. 1, 1999, pp. 188–196.

[14]Tan, Z. M., and Hsu, P.-F., "An Integral Formulation of Transient Radiative Transfer—Theoretical Investigation," 34th National Heat Transfer Conf., Paper NHTC2000-12077, Aug. 2000.

[15]Wu, C.-Y., and Wu, S.-H., "Integral Equation Formulation for Transient Radiative Transfer in an Anisotropically Scattering Medium," *International Journal of Heat and Mass Transfer*, Vol. 43, No. 11, 2000, pp. 2009–2020.

[16]Guo, Z., and Kumar, S., "Radiation Element Method for Transient Hyperbolic Radiative Transfer in Plane-Parallel Inhomogeneous Media," *Numerical Heat Transfer B*, Vol. 39, No. 4, 2001, pp. 371–387.

[17]Guo, Z., and Kumar, S., "Discrete Ordinates Solution of Short-Pulsed Laser Transport in Two-Dimensional Turbid Media," *Applied Optics*, Vol. 40, No. 19, 2001, pp. 3156–3163.

[18]Howell, J. R., "The Monte Carlo Method in Radiative Heat Transfer," *Journal of Heat Transfer*, Vol. 120, No. 2, 1998, pp. 547–560.

[19]Fiveland, W. A., "Three-Dimensional Radiative Heat Transfer Solutions by the Discrete-Ordinates Method," *Journal of Thermophysics and Heat Transfer*, Vol. 2, No. 4, 1988, pp. 309–316.

[20]Raithby, G. D., and Chui, E. H., "A Finite-Volume Method for Predicting a Radiant Heat Transfer in Enclosures with Participating Media," *Journal of Heat Transfer*, Vol. 112, No. 2, 1990, pp. 415–423.

[21]Hsu, P.-F., and Farmer, J. T., "Benchmark Solution of Radiative Heat Transfer Within Nonhomogeneous Participating Media Using the Monte Carlo and YIX Method," *Journal of Heat Transfer*, Vol. 119, No. 1, 1997, pp. 185–188.

[22]Menguc, M. P., and Viskanta, R., "Radiative Transfer in Three-Dimensional Rectangular Enclosures Containing Inhomogeneous, Anisotropically Scattering Media," *Journal of Quantitative Spectroscopy and Radiatative Transfer*, Vol. 33, No. 6, 1985, pp. 533–549.

[23]Maruyama, S., and Guo, Z., "Radiative Heat Transfer in Arbitrary Configurations with Nongray Absorbing, Emitting, and Anisotropic Scattering Media," *Journal of Heat Transfer*, Vol. 121, No. 3, 1999, pp. 722–726.

[24]Modest, M. F., *Radiative Heat Transfer*, McGraw-Hill, New York, 1993, Chap. 15.

[25]Fiveland, W. A., 1991, "The Selection of Discrete Ordinate Quadrature Sets for Anisotropic Scattering," *Fundamentals of Radiation Heat Transfer*, HTD-Vol. 72, American Society of Mechanical Engineers, Fairfied, NJ, No. 4, 1991, pp. 89–96.

[26]Ozisik, M. N., *Heat Conduction*, Wiley, New York, 1980, Chap. 5.

[27]Lathrop, K. D., "Spatial Differencing of the Transport Equation: Positive vs Accuracy," *Journal of Computational Physics*, Vol. 4, No. 4, 1968, pp. 475–498.

[28]Anderson, D. A., Tannehill, J. C., and Pletcher, R. H., *Computational Fluid Mechanics and Heat Transfer*, Hemisphere, New York, 1984, Chap. 4.

[29]Lathrop, K. D., and Brinkley, F. W., "TWOTRAN-II Code," Los Alamos National Lab., Rept. LA-4848-MS, Los Alamos, NM, 1973.